

LaST₀: Latent Spatio-Temporal Chain-of-Thought for Robotic Vision–Language–Action Model

Zhuoyang Liu^{1,2,4*}, Jiaming Liu^{1,4*†}, Hao Chen^{3,4*}, Ziyu Guo³, Chengkai Hou^{1,2}, Chenyang Gu¹, Jiale Yu¹, Xiangju Mi¹, Renrui Zhang³, Zhengping Che^{2†}, Jian Tang², Pheng-Ann Heng³, Shanghang Zhang^{1✉}

¹State Key Laboratory of Multimedia Information Processing, School of Computer Science, Peking University, ²Beijing Innovation Center of Humanoid Robotics, ³CUHK, ⁴Simplexity Robotics

*Equal contribution, †Project lead, ✉Corresponding author

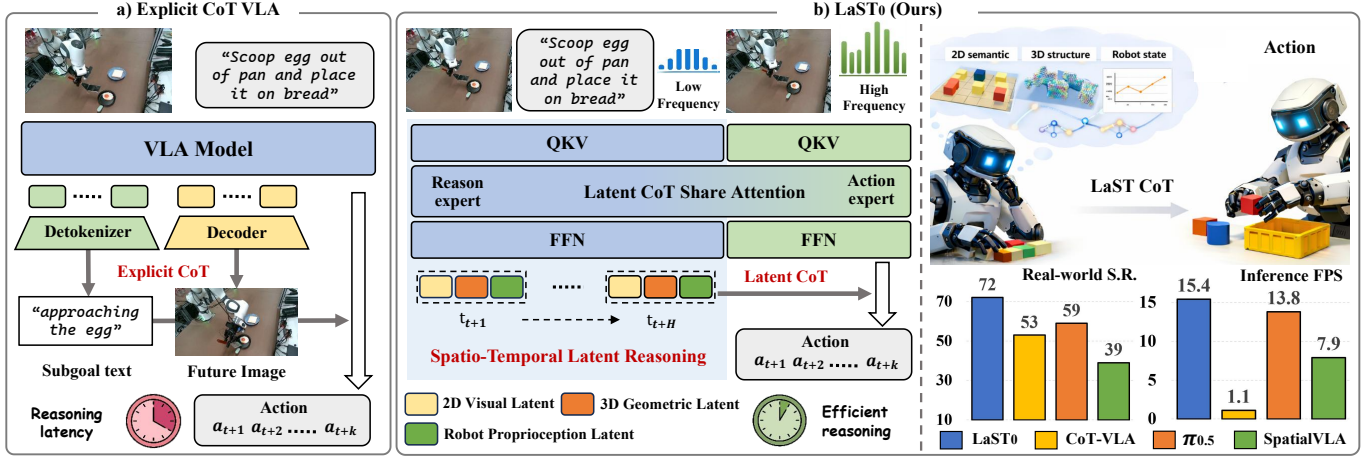


Fig. 1: **Overview.** (a) Unlike previous VLA methods that seek to improve manipulation by explicitly generating linguistic reasoning traces or future visual observations, (b) we propose LaST₀, a framework that enables efficient reasoning before acting through a Latent Spatio-Temporal CoT. This latent CoT captures multimodal physical and robotic dynamics that are difficult to verbalize and propagates them over time to form temporally consistent reasoning trajectories. LaST₀ achieves SOTA performance across a wide range of real-world and simulated tasks, while supporting real-time model inference.

Abstract—Vision–Language–Action (VLA) models have recently demonstrated strong generalization capabilities in robotic manipulation. Some existing VLA approaches attempt to improve action accuracy by explicitly generating linguistic reasoning traces or future visual observations before action execution. However, explicit reasoning typically incurs non-negligible inference latency, which constrains the temporal resolution required for robotic manipulation. Moreover, such reasoning is confined to the linguistic space, imposing a representational bottleneck that struggles to faithfully capture ineffable physical attributes. To mitigate these limitations, we propose LaST₀, a framework that enables efficient *reasoning before acting* through a Latent Spatio-Temporal Chain-of-Thought (CoT), capturing fine-grained physical and robotic dynamics that are often difficult to verbalize. Specifically, we introduce a token-efficient latent CoT space that models future visual dynamics, 3D structural information, and robot proprioceptive states, and further extends these representations across time to enable temporally consistent implicit reasoning trajectories. Furthermore, LaST₀ adopts a dual-system architecture implemented via a Mixture-of-Transformers design, where a reasoning expert conducts low-frequency latent inference and an acting expert generates

high-frequency actions conditioned on robotics-oriented latent representations. To facilitate coordination, LaST₀ is trained with heterogeneous operation frequencies, enabling adaptive switching between reasoning and action inference rates during deployment. Across ten simulated and six real-world manipulation tasks, LaST₀ improves mean success rates by 8% and 13% over prior VLA methods, respectively, while achieving substantially faster inference. Moreover, LaST₀ demonstrates strong long-horizon robustness, attaining nearly a 5× higher success rate at the final step of a multi-step real-world task. Project website: <https://sites.google.com/view/last0>

I. INTRODUCTION

Recently, robot imitation learning has emerged as a dominant paradigm for acquiring manipulation policies from expert demonstrations [25, 16, 72]. By inheriting the semantic understanding and common-sense reasoning capabilities of Vision–Language Models (VLMs) [1, 40, 75, 20], Vision–Language–Action (VLA) models integrate rich pretrained knowledge with the low-level control capabilities of robotic

policies [7, 5, 50, 35]. This integration endows robotic agents with a unified framework for interpreting human instructions and executing corresponding manipulation primitives in dynamic environments.

Rather than simply mapping observations to actions, recent advances in VLA models have been inspired by the Chain-of-Thought (CoT) reasoning paradigm in general VLMs [30, 89]. In this line of work, some approaches enhance manipulation stability and interpretability by explicitly generating linguistic reasoning traces or affordance representations [85, 46]. In parallel, other studies seek to capture environmental dynamics by predicting future states, such as subgoal images or camera-view depth maps [71, 90, 77, 92, 52]. Despite their demonstrated benefits, explicit CoT VLA methods remain constrained by two fundamental challenges in robotic manipulation. **On the one hand**, explicit reasoning typically incurs non-negligible inference latency. The autoregressive generation paradigm introduces inevitable computational overhead [69, 76], limiting the VLA model’s ability to achieve real-time responsiveness. This latency further restricts VLA models from reasoning effectively along the temporal dimension, thereby undermining the temporal consistency required for closed-loop manipulation. **On the other hand**, explicit reasoning is often confined to the linguistic space, imposing a representational bottleneck that struggles to faithfully capture ineffable physical attributes. In contrast, robotic agents must reason about and interact with the physical world, which is essential for robust manipulation in a dynamic environment.

In this paper, we propose **LaST**₀, a dual-system VLA model that enables efficient reason-before-act behavior through a **Latent Spatio-Temporal Chain-of-Thought** (CoT). As shown in Fig. 1, unlike prior explicit CoT-based VLA methods, LaST₀ performs reasoning in a compact latent space, enabling the capture of fine-grained physical and robotic dynamics that are difficult to verbalize, while supporting temporally coherent modeling for closed-loop manipulation. Specifically, we introduce a token-efficient latent CoT space that autoregressively predicts future latent tokens of 2D images, 3D point clouds, and proprioceptive states. As a result, the VLA model can implicitly model the semantic and geometric structure of physical dynamics, while forming an internal representation of the robot state, thereby capturing the relationship between the robot and its interactive environment. Meanwhile, the latent CoT space is extended across future keyframes, enabling temporally consistent causal reasoning, which improves action coherence in closed-loop robotic manipulation. Although the proposed latent CoT is compact and encodes richer physical information, incorporating it into action generation still introduces additional inference overhead. Therefore, leveraging temporally extended latent conditions, we further propose a dual-system architecture implemented via a Mixture-of-Transformers (MoT) design, as shown in Fig. 1. Specifically, two experts are integrated within a single VLA model: a slow reasoning expert, which performs low-frequency latent inference to capture spatio-temporal dependencies, and a fast acting expert, which generates actions conditioned on high-frequency

observations and periodically updated latent representations. Through shared self-attention mechanisms, LaST₀ enables long-context interaction between the latent CoT space and the action space, thereby effectively coordinating deliberative reasoning with responsive control.

For the training procedure, both the latent reasoning expert and the action expert are initialized from the same pretrained multimodal foundation model (i.e., Janus-Pro [12]). We then perform large-scale pretraining of LaST₀ on diverse robotic manipulation datasets [62, 41, 82], ensuring a shared representation space and seamless interaction between the two experts within a unified VLA model. During downstream training, we first optimize the slow reasoning expert via supervised fine-tuning using ground-truth latent representations extracted from auxiliary encoders. This latent-space teacher forcing establishes a reliable latent scaffold for subsequent action learning. Afterward, the reasoning expert is frozen, and the action expert is trained under heterogeneous fast–slow operating ratios, enabling the VLA model to adaptively select different frequencies during deployment. For evaluation, we systematically assess LaST₀ on 10 simulated tasks and six complex real-world tasks, including single-arm and dual-arm settings. Across these benchmarks, LaST₀ outperforms prior state-of-the-art (SOTA) VLA methods by 8% and 13%, respectively, while achieving a 14× speedup over previous explicit CoT VLA approaches. In addition, we validate the closed-loop manipulation capability of LaST₀ on long-horizon real-world tasks under dynamic conditions. Notably, the robot is able to repeatedly and continuously scoop eggs from a pan while adapting to dynamic environmental changes, demonstrating robust spatio-temporal understanding. Our contributions are summarized as follows:

- We propose **LaST**₀, a unified VLA model that enables efficient reason-before-act behavior through a **Latent Spatio-Temporal CoT**, performing reasoning in a compact latent space to capture fine-grained physical and robotic dynamics that are difficult to verbalize.
- We design a spatio-temporal latent CoT space for manipulation, which autoregressively models future semantic, geometric, and proprioceptive information, allowing **LaST**₀ to reason about physical dynamics in a temporally coherent manner.
- We introduce a dual system VLA architecture, implemented via MoT scheme, that coordinates low-frequency latent reasoning with high-frequency action generation, enabling real-time robotic manipulation.

II. RELATED WORK

A. Vision-Language-Action Model

Vision-Language-Action (VLA) models have rapidly advanced as an effective paradigm for instruction-conditioned robotic manipulation, primarily driven by scaling robot demonstration data and adapting pretrained VLMs for robotic control [6, 7, 3, 48, 42]. To improve expressivity for continuous actions, recent VLA research has increasingly employed continuous generative policy heads. Diffusion-based

VLA [51, 79, 81, 50] models complex action distributions through iterative denoising, while flow-matching formulations [5, 35, 22, 4, 80] offer an alternative that can improve sampling efficiency and stability. These directions aim to leverage the generalization of VLMs to specifically enhance the controllability, precision, and fidelity of continuous action generation. Beyond imitation learning, more work explores post-training VLA models via Reinforcement Learning (RL) to enhance robustness. Offline methods leverage preference-based alignment [91] to steer policies using static data without requiring simulation. Online RL methods [70, 15, 14, 44, 54] refine policies through active environment interaction. However, scaling RL-based strategies for open-world manipulation remains constrained by challenges in sample efficiency and training stability. Meanwhile, recent research equips VLA models with “reason-before-act” components to retain accurate representations of the dynamic environment and improve action quality. [35, 49, 86] adopts textual chain-of-thought (CoT) generation for future task planning and action generation. Subsequent work [78, 92, 10, 26, 8, 90] extends generative text planning to future image prediction. Furthermore, in order to model fine-grained future states, [52, 9, 28] introduces predictions of future multi-modal information. However, explicit reasoning typically incurs non-negligible inference latency, thereby limiting the VLA model’s ability to achieve real-time responsiveness. Unlike explicit CoT-based VLA methods, LaST₀ employs a latent spatio-temporal CoT strategy to efficiently capture fine-grained physical and robotic dynamics within a compact latent space.

B. Latent Chain-of-Thought

Recent work of VLM in the general domain [13, 23, 31, 84, 76] has explored latent CoT reasoning to address the limitations of explicit CoT on ineffable visual-spatial matching and high-cost text or image generation. These methods perform multi-step inference directly in continuous latent spaces, allowing intermediate reasoning to be compact, implicit, and tightly integrated with downstream prediction. Beyond general-purpose VLMs, similar approaches have been adopted in the embodied intelligence domain, where textual CoT is particularly ill-suited for representing low-level signal generation. LCDrive [69] replaces language-based explanations with action-aligned latent rollouts, allowing the model to simulate future outcomes and evaluate alternatives directly in the action space. Meanwhile, Thinkact [34] compresses intermediate motion plans into compact representations to guide action generation. Prior latent CoT frameworks mainly operate on textual reasoning or abstract 2D representations for general tasks. In contrast, LaST₀ is tailored for robotic manipulation, where the VLA model reasons in a physically grounded latent space that jointly encodes semantic intent, geometric structure, and robot state, thereby capturing the embodied interaction between the robot and its environment.

III. METHOD

In Section III-A, we describe the preliminaries of VLA models and contrast explicit and latent Chain-of-Thought (CoT) paradigms in the robotic domain. The proposed LaST₀ with a Mixture-of-Transformers (MoT) architecture, featuring dual experts coupled via a shared attention mechanism, is detailed in Section III-B. Section III-C elucidates the construction of our spatio-temporal latent space, explaining the encoding and compression of future physical knowledge. We then describe the fast–slow system design and its asynchronous inference frequencies in Section III-D. Finally, Section III-E outlines the complete training paradigm, from large-scale pretraining to supervised fine-tuning.

A. Preliminaries

VLA Problem Formulation. We formulate the robot manipulation task as a probabilistic sequence decision-making problem [42]. At each timestep t , the policy receives a natural language instruction l_t and visual observations $I_t \in \mathbb{R}^{H \times W \times 3}$ that capture the current environment. The objective of the VLA model π_θ is to generate an optimal action sequence $\mathbf{a}_{t:t+H}$ conditioned on the instruction l_t . Consistent with prior works [50, 5], we define the action space within the Special Euclidean group $SE(3)$. For single-arm configurations (e.g., Franka research 3), we employ a 7-DoF end-effector pose control mechanism, formulated as $\mathbf{a}_t \in \mathbb{R}^7$. Specifically, this control vector consists of 3-DoF for relative positional offsets ($[\Delta x, \Delta y, \Delta z] \in \mathbb{R}^3$), 3-DoF for rotation (represented as Euler angles [roll, pitch, yaw] $\in \mathbb{R}^3$), and 1-DoF for the gripper state (open/closed, $g \in \mathbb{R}^1$). For dual-arm configurations, to validate our model’s scalability, we extend this to a 14-DoF representation by concatenating the control signals.

Robotic CoT Reasoning. To bridge the gap between high-level visual observations and low-level control, recent VLA methods introduce an intermediate CoT variable \mathcal{Z} . This formulation decomposes the policy distribution into a reasoning stage (predicting \mathcal{Z}) and an execution stage (predicting \mathbf{a} conditioned on \mathcal{Z}):

$$p(\mathbf{a}, \mathcal{Z} | I_t, l) = p(\mathbf{a} | \mathcal{Z}, I_t, l) \cdot p(\mathcal{Z} | I_t, l)$$

Existing methods typically adopt an explicit CoT paradigm, where \mathcal{Z} consists of discrete natural language tokens [45] or image tokens [92, 88]. While interpretable, these approaches confine reasoning to the linguistic space of LLMs, which struggles to represent ineffable physical attributes and incurs inference latency due to explicit decoding. To overcome these limitations, we propose a new latent CoT paradigm for the robotic domain. Unlike explicit CoT, we define $\mathcal{Z} = \{\mathbf{z}_1, \dots, \mathbf{z}_k\}$ as a sequence of continuous embeddings in a high-dimensional latent space. In our framework, the latent variable \mathcal{Z} is trained to autoregressively predict future dynamics, including latent representations of 2D images, 3D point clouds, and robot proprioceptive states, thereby modeling the physical world in a compact space.

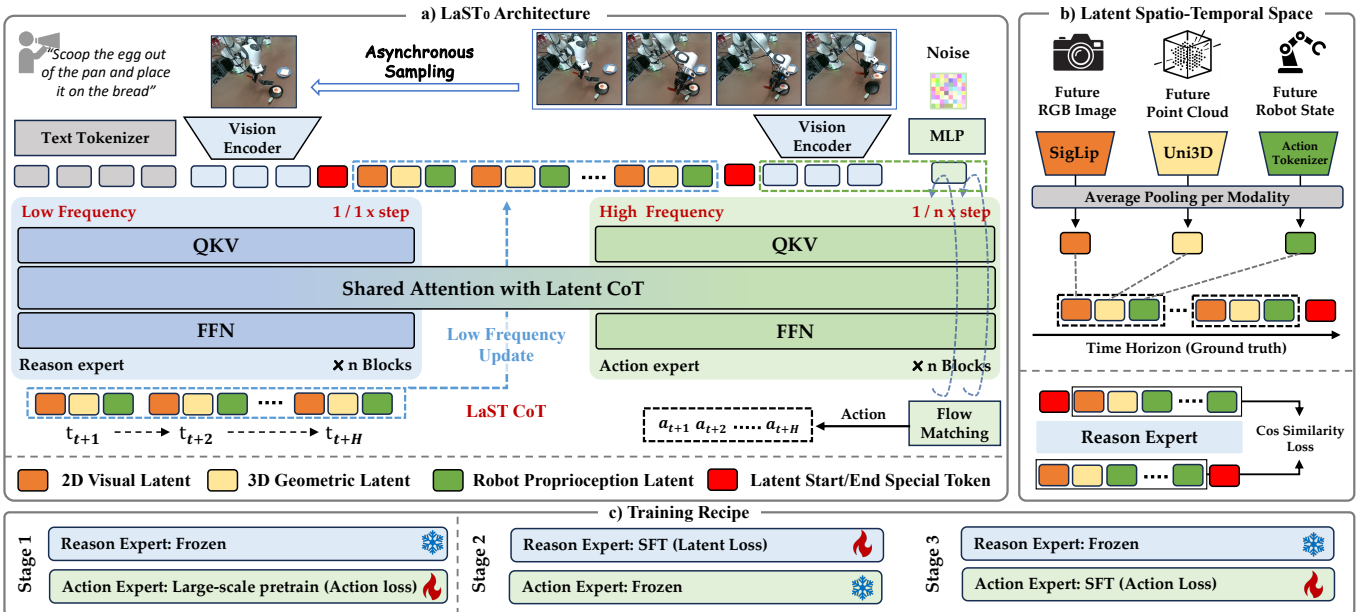


Fig. 2: **Overall framework of LaST₀.** **a)** We propose LaST₀, a unified VLA model with a dual-system architecture. The model is implemented via a MoT scheme with two experts interacting through shared self-attention. The slow reasoning expert operates at a low frequency, taking visual observations and text as input to construct the Last CoT by autoregressively predicting spatio-temporal latent tokens, which are stored in the KV cache. The fast acting expert operates at a higher frequency and generates actions via flow matching, conditioned on high-frequency observations and periodically updated latent representations. **b)** We design a spatio-temporal latent space tailored for the reasoning expert, where pretrained modality-specific encoders extract features from future RGB images, point clouds, and robot states at keyframes. These features serve as ground-truth latent CoT targets for supervising the reasoning expert. **c)** The training procedure consists of three stages with different parameter update strategies, ensuring a reliable latent and robust action generation.

B. LaST₀ Architecture

Overview. As illustrated in Fig. 2 a), we elaborate on the architectural of LaST₀. Our model is initialized on the Janus-Pro[12], utilizing DeepSeek-LLM 1B as the backbone. To bridge the gap between reasoning and control, we transform this standard decoder-only transformer into a unified MoT dual-system architecture, constructing the "reason-before-act" paradigm. This design enables the model to effectively decouple the generation of slow, high-level latent reasoning from fast, low-level action execution, while maintaining seamless information flow through a shared attention mechanism.

Vision Encoder. For each input RGB observation $I_t \in \mathbb{R}^{H \times W \times 3}$ ($H = W = 224$), we employ SigLIP-Large[87] to extract semantic features. Following standard practices, the image is divided into non-overlapping patches of size 14×14 , which are then flattened and linearly projected. This process yields a compact feature sequence $f_{\text{img}} \in \mathbb{R}^{B \times N_{\text{img}} \times d_v}$, where B denotes the batch size, N_{img} represents the sequence length, and d_v is the embedding dimension. In our framework, these encoded features f_{img} serve a dual purpose: the current frame acts as real-time contextual input to the MoT experts, while future frames provide ground-truth target embeddings for the visual component of the latent CoT.

Point Cloud Encoder (training only). To equip the model with fine-grained geometric perception and robust 3D spatial reasoning, we integrate a pretrained point cloud encoder that

explicitly captures object geometry and spatial knowledge. We adopt Uni3D [94], a scalable 3D foundation model, which has been pre-trained on massive 3D datasets to align point cloud features with image and text embeddings. Note that, unlike the vision encoder, the point cloud encoder is not used during inference. Instead, Uni3D is solely employed to encode ground-truth point clouds into compact 3D feature representations within the latent CoT space.

Mixture-of-Transformers LLM Backbone. We adopt DeepSeek-LLM 1B as our foundation, repurposing its 24-layer decoder-only transformer architecture into a unified dual-system policy. Inspired by [21], to efficiently support both high-level reasoning and low-level execution, we transform the standard backbone into a MoT architecture. Unlike conventional transformers that apply a homogeneous set of weights to all tokens, our MoT design introduces task-specific parameter sets for all non-embedding components, including Feed-Forward Networks (FFN), attention projections (W_Q, W_K, W_V, W_O), and Layer Normalizations, while maintaining a shared global self-attention context. This modification essentially yields two specialized experts residing within the same $d = 2048$ dimensional latent space, while a slow reasoning expert responsible for autoregressively synthesizing the Latent CoT embeddings \mathcal{Z} from language and slow-stream visual inputs, and a fast acting expert dedicated to generating high-frequency actions \mathbf{a}_t . The design of different operating

frequencies for the two experts is described in Section III-D.

MLP Components. To further clarify the LaST₀ architecture, we describe the remaining auxiliary components, all of which are implemented as Multi-Layer Perceptrons (MLPs). First, a 3D Projector aligns point cloud features to the same dimension, serving as supervise targets for the Latent CoT. Regarding the action generation mechanism, given that our fast acting expert adopts a Flow Matching policy [5], specific modules are incorporated to handle the continuous generative dynamics. For the action expert input, we use a timestep MLP to encode the continuous time coordinate $t \in [0, 1]$, initialized with sinusoidal embeddings, and a noised-action MLP to project the perturbed action state. For the action expert output, a projector MLP is used to transform the predicted flow velocity field, enabling the model to generate precise actions.

C. Latent Spatio-Temporal Chain-of-Thought

To capture fine-grained physical and robotic dynamics that are difficult to verbalize, while enabling efficient temporal modeling for manipulation, we construct a Latent Spatio-Temporal Chain-of-Thought (LaST CoT).

Latent Embedding Construction. To model temporal environmental dynamics, our latent representation encodes multimodal future states over a horizon H . As shown in Fig. 2 b), for each future timestep $k \in \{1, \dots, H\}$, we extract features from three complementary modalities to form a holistic physical representation. Future RGB frames I_{t+k} are encoded into visual latents z_k^v using the frozen SigLIP-Large encoder; simultaneously, future point clouds P_{t+k} are processed by the Uni3D encoder to yield geometric latents z_k^p capturing 3D spatial occupancy, while future robot states s_{t+k} are transformed into proprioceptive latents z_k^s via an action tokenizer. Together, these representations enable the VLA model to implicitly model the semantic and geometric structure of physical dynamics, while maintaining an internal estimate of the robot’s state, thereby capturing the interaction between the robot and its environment. To ensure high inference efficiency, we apply average pooling to compress the feature maps of each modality into a single representative token. This results in a compact set of embeddings $\{z_k^v, z_k^p, z_k^s\}$ for each step. We then organize these tokens in an interleaved, chronological order to preserve causal physical dependencies:

$$\mathcal{Z}_{\text{GT}} = [z_1^v, z_1^p, z_1^s, z_2^v, z_2^p, z_2^s, \dots, z_H^v, z_H^p, z_H^s]. \quad (1)$$

By fusing visual information, 3D geometric structure, and robot proprioception, the model develops a holistic understanding of both the physical world and the robot itself. The interleaved multimodal structure further encourages the model to learn the coupled dynamics across different modalities over time. Notably, the temporal granularity can be flexibly adjusted: we either adopt keyframe extraction as in [67] or use densely sampled frames, depending on task requirements. Moreover, by compressing high-dimensional sensory inputs into a latent sequence of length $3 \times H$, we avoid the prohibitive cost of decoding pixel-level images or long textual sequences. As discussed in Section III-D, we introduce an asynchronous

frequency design for the two experts, which further accelerates action generation.

Sequence Structure. To better organize LaST CoT reasoning and action generation, we introduce three special tokens: $\langle \text{latent_start} \rangle$, $\langle \text{latent_end} \rangle$, and a placeholder token $\langle \text{latent_pad} \rangle$. The reasoning segment is structurally defined as a sequence bounded by the start and end tokens, with the intermediate positions reserved for the latent embeddings. During Training, we replace the intermediate $\langle \text{latent_pad} \rangle$ tokens with the ground-truth latent sequence \mathcal{Z}_{GT} . This allows the model to learn the transition dynamics via standard teacher forcing. While during Inference, the model is initialized with $\langle \text{latent_start} \rangle$ followed by a sequence of $\langle \text{latent_pad} \rangle$ tokens. The slow reason expert then autoregressively generates continuous embeddings, sequentially filling the positions of the $\langle \text{latent_pad} \rangle$ placeholders until the pre-defined horizon is filled. The horizon length can be adaptively adjusted, and its effect is further analyzed through ablation studies.

Latent Supervision Strategy. We train the slow reasoning expert to predict latent CoT embeddings in an autoregressive manner, using continuous latent regression rather than discrete token likelihoods [84, 76]. Specifically, the slow expert is trained to predict a sequence of latent reasoning states $\hat{\mathcal{Z}}$ in a next-step prediction manner, conditioned on preceding observations and context. Unlike conventional CoT supervision based on discrete token prediction, our latent targets consist of continuous, high-dimensional embeddings that encode future physical world states. To align the predicted latent semantics with the ground-truth representations, we employ cosine similarity as the supervision objective. The loss is defined as:

$$\mathcal{L}_{\text{latent}} = \sum_{t=1} \left(1 - \frac{\hat{\mathbf{z}}_t \cdot \mathbf{z}_t^{\text{GT}}}{\|\hat{\mathbf{z}}_t\| \|\mathbf{z}_t^{\text{GT}}\|} \right). \quad (2)$$

By maximizing directional alignment in the latent space, this objective encourages the model to anticipate future physical dynamics in a structured and compact manner. The slow expert learns a physically grounded latent reasoning trajectory that serves as a stable scaffold for the action generation.

D. Dual-System Coordination

Asynchronous Frequency Coordination. To coordinate LaST CoT reasoning with high-frequency robotic control, we introduce an asynchronous frequency mechanism between the slow reasoning expert and the fast acting expert. As shown in Fig. 3, we decouple their operating frequencies by a fixed update ratio κ (e.g., $\kappa \in \{2, 4, 8\}$). The slow expert is activated only at sparse keyframes ($t \bmod \kappa = 0$), where it performs autoregressive latent CoT reasoning. In contrast, the fast expert runs at the native control frequency and remains active at every timestep. Between consecutive keyframes ($t \bmod \kappa \neq 0$), the slow reasoning expert is held dormant, while the fast expert generates actions by conditioning on the most recent latent reasoning output. This strategy ensures that action generation is continuously guided by stable, temporally consistent

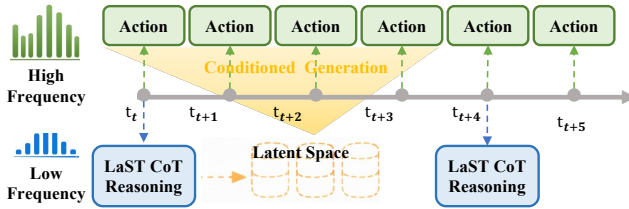


Fig. 3: The slow reasoning expert performs low-frequency latent CoT reasoning to capture long-horizon spatio-temporal dependencies, while the fast acting expert generates actions conditioned on high-frequency observations and periodically updated latent knowledge. Benefiting from training with a mixture of fast–slow operating ratios, the model can flexibly adjust the reasoning–action frequency ratio at test time.

latent conditions, while minimizing redundant computations for LaST CoT reasoning.

For the inputs to the two experts, the slow reasoning expert receives the natural language instruction l and the low-frequency observation I_{slow} , constructing the Latent CoT that encapsulates future physical dynamics. Conversely, the fast acting expert is optimized for rapid closed-loop feedback and receives only the high-frequency observation I_{fast} . Crucially, since our MoT architecture maintains a unified token sequence, the fast expert can efficiently attend to both the linguistic goal and the Latent CoT tokens via the shared attention mechanism.

Inference via KV Cache. During inference, the Key-Value states computed by the slow expert (encapsulating the Latent CoT) are cached in memory. During intermediate fast-control steps, the acting expert only encodes the current observation and attends to the frozen latent CoT cache, effectively retrieving the CoT tokens with $O(1)$, without re-invoking the slow reasoning process. This approach eliminates repetitive decoding, allowing our model to achieve an inference speed of 15.4 Hz on a single RTX 4090 GPU when operating with a 1:4 fast–slow frequency ratio.

E. Training Recipe

Large-Scale Robotic Pretraining. Both the latent reasoning expert and the action expert are initialized from the Janus-Pro 1B foundation model. As shown in Fig. 2 c), Stage 1 performs large-scale pretraining on a diverse corpus of over 400K trajectories aggregated from Open-X-Embodiment [62], DROID [41], ROBOMIND [82, 33], and other robotic datasets. Notably, beyond following prior VLA works in applying data quality filtering [42, 52], we additionally ensure that all robot state annotations are accurate and physically consistent. Detailed statistics and descriptions of the pretraining data are provided in Appendix A. This stage optimizes the model on broad robotic datasets to establish a shared representation space, enabling seamless interaction between reasoning and execution within the unified VLA framework.

Supervised Fine-Tuning (SFT). As shown in Fig. 2, we employ a decoupled 2-stage SFT in downstream adaptation, aiming to prevent the catastrophic forgetting of reasoning capabilities when training action expert. In stage 2, we first

optimize the slow reasoning expert while freezing the action expert. By exclusively optimizing the Latent CoT regression loss $\mathcal{L}_{\text{latent}}$, the slow expert aligns its latent representations with domain-specific physical dynamics. Subsequently, in stage 3, we freeze the converged slow expert and load the robotic data pretrained weights for the fast expert. The fast acting expert is subsequently fine-tuned using the standard Flow Matching loss $\mathcal{L}_{\text{flow}}$. While the loss formulation and noise injection scheme follow π_0 [5], our approach differs in that the entire LLM is directly used as the action denoising model, without introducing any additional action heads. Meanwhile, the action expert is trained with randomly mixed fast–slow operating ratios (e.g., 1:1, 1:2, 1:4), which exposes it to latent conditions updated at varying delays. As a result, LaST₀ can flexibly accommodate different reasoning–update frequencies at deployment and adaptively choose the fast–slow inference rate. In ablation studies, we find that training with mixed fast–slow operating ratios does not degrade performance; instead, it improves the model’s robustness during inference.

IV. EXPERIMENT

In Section IV-A, we evaluate the manipulation performance and inference efficiency of LaST₀ against prior methods in simulated environments. The contribution of each component is analyzed through ablation studies in Section IV-B. Section IV-C presents both quantitative and qualitative results of LaST₀ on real-world manipulation tasks, including single-arm and dual-arm control under diverse robot configurations.

A. Simulation Experiment

Data collection. We evaluate LaST₀ on a diverse set of 10 manipulation tasks from the RLBench [36] benchmark, conducted in the CoppeliaSim simulation environment. The evaluated tasks include 1) *Close box*, 2) *Close Laptop*, 3) *Toilet seat down*, 4) *Sweep to dustpan*, 5) *Close fridge*, 6) *Phone on base*, 7) *Take umbrella out*, 8) *Frame off hanger*, 9) *Wine at rack*, and 10) *Water plants*. All tasks are executed using a Franka Panda robotic arm with a single front-view observation. Demonstration data are collected by following pre-defined waypoints with motion plans generated via the Open Motion Planning Library [68]. Following the frame-sampling protocol adopted in prior work [67, 27, 38], we construct a training dataset comprising 100 demonstration trajectories per task.

Training and evaluation protocol. We benchmark LaST₀ against six representative state-of-the-art VLA models: Open-VLA [42], $\pi_{0.5}$ [35], CogACT [47], SpatialVLA [64], CoT-VLA [92] and HybridVLA [50]. For all baselines, we initialize from the officially released pretrained checkpoints and follow the full fine-tuning configurations recommended by the paper. For CoT-VLA, we reimplement the method on top of Janus-Pro [12], the same foundation model used in our approach, and reproduce its explicit CoT reasoning to ensure a fair comparison. For LaST₀, each observation consists of a single RGB image resized to 384×384 , a point cloud uniformly subsampled to 1024 points, a language instruction obtained directly from the simulator, and the robot proprioceptive state

TABLE I: **Comparison of LaST₀ and baselines on RLBench.** All methods are trained in the multi-task setting [67], and we report mean success rates (S.R.). Inference speed is evaluated on an NVIDIA 4090 GPU.

Models	Close box	Close laptop lid	Toilet seat down	Sweep to dustpan	Close fridge	Phone on base	Umbrella out	Frame off hanger	Wine at rack	Water plants	Mean S.R. \uparrow & Var \downarrow	Infer. speed \downarrow
OpenVLA [42]	0.60	0.35	0.75	0.55	0.85	0.20	0.30	0.15	0.20	0.05	0.40 \pm 0.02	6.3 Hz
SpatialVLA [64]	0.80	0.70	0.85	0.20	0.80	0.15	0.25	0.40	0.15	0.30	0.46 \pm 0.03	7.9 Hz
CogACT [47]	0.90	0.80	0.95	0.50	0.85	0.50	0.55	0.45	0.30	0.25	0.61 \pm 0.04	9.8 Hz
CoT-VLA [92]	0.95	0.75	1.00	0.80	0.65	0.50	0.40	0.50	0.55	0.50	0.66 \pm 0.03	1.1 Hz
$\pi_{0.5}$ [35]	0.90	0.95	0.85	0.75	1.00	0.05	0.10	0.80	0.75	0.35	0.65 \pm 0.04	13.8 Hz
HybridVLA [50]	0.85	0.95	1.00	0.90	1.00	0.50	0.50	0.70	0.50	0.50	0.74 \pm 0.04	6.1 Hz
LaST ₀	0.95	0.95	1.00	0.80	0.85	0.75	0.75	0.70	0.85	0.65	0.82 \pm 0.03	15.4 Hz

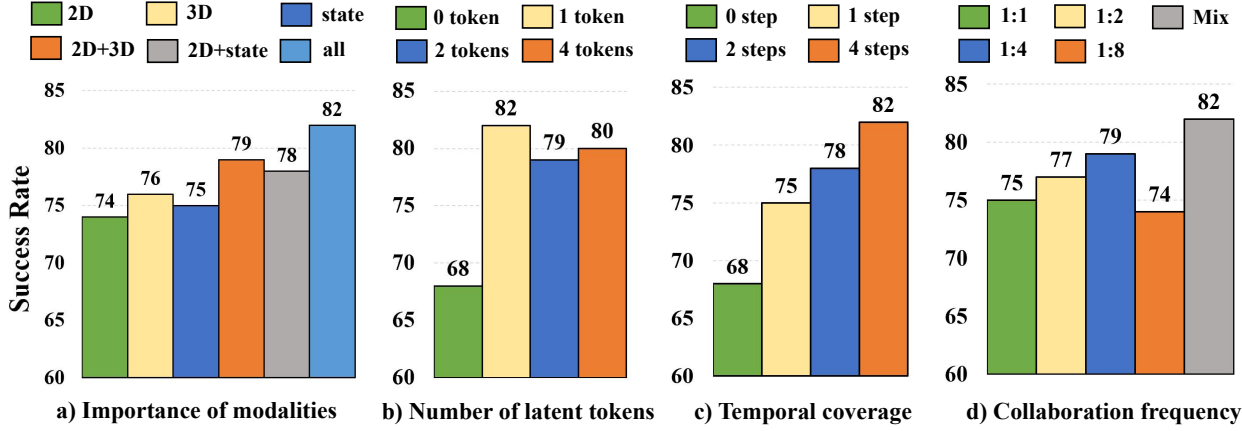


Fig. 4: **Ablation study on key design choices of LaST₀.** We analyze (a) the importance of different latent modalities, (b) the number of tokens allocated per latent modality, (c) the temporal coverage in latent reasoning, and (d) the collaboration frequency between reasoning and action experts. Results are reported as average success rates across 10 RLBench tasks, demonstrating the contribution of each component to overall performance.

synchronized with the predicted action. Note that point cloud data are used exclusively during training to construct latent ground truth and are not needed during inference. The model is trained for 40 epochs in Stage 2 and 300 epochs in Stage 3, using the AdamW optimizer [53] across 8 NVIDIA A800 GPUs. Evaluation follows the protocol of prior work [47, 27]. For each task, we perform 20 rollout trials using the final checkpoint, repeat the evaluation three times with different random seeds, and report the mean success rate together with its variance.

Quantitative analysis. As summarized in Table I, LaST₀ achieves a mean success rate of 82% across 10 RLBench manipulation tasks, substantially outperforming all prior baselines. In particular, LaST₀ surpasses the strongest existing methods, HybridVLA-7B (74%), $\pi_{0.5}$ -3B (65%), and CogACT-7B (61%), by margins of 8%, 17%, and 21%, respectively. Beyond the overall average, LaST₀ attains the highest success rate on 7 out of 10 tasks, indicating consistent performance gains across diverse manipulation skills, while also showing relatively low variance (± 0.03), reflecting stable execution across tasks. These improvements primarily stem from the latent reasoning representations produced by the reasoning expert, which condition the action expert with compact latent states encoding future visual dynamics, 3D spatial structure, and robot proprioceptive information, enabling more stable and temporally coherent action generation. In terms of

execution efficiency, LaST₀ operates at an inference speed of 15.4 Hz with an action chunk size of one, which is significantly faster than explicit CoT methods (CoT-VLA: 1.1 Hz) and remains competitive with $\pi_{0.5}$ (13.8 Hz). This demonstrates that LaST₀ achieves superior task performance without sacrificing real-time control efficiency. Moreover, as shown in Fig. 5, we compare the attention heatmaps of LaST₀ against variants without CoT and with explicit CoT (CoT-VLA). While the no-CoT variant and the explicit CoT method fail to aggregate features on the manipulated objects and ignore the relationship between the robot and the manipulated objects, LaST₀ exhibits a highly concentrated attention pattern, highlighting its superior understanding of spatio-temporal information in downstream tasks.

B. Ablation Study

To validate the key design choices of LaST₀, we conduct comprehensive ablation experiments on 10 RLBench tasks, using the same training and evaluation settings as in the simulation experiments. The results are summarized as follows.

Importance of latent CoT modalities. As shown in Fig. 4 a), we analyze the contribution of each latent modality by selectively ablating individual latent components while keeping the overall architecture unchanged. When using only the image, point cloud, or robot state latent, the model achieves success rates of 74%, 76%, and 75%, respectively, indicating

TABLE II: **Comparison of LaST₀ and baselines in real-world manipulation tasks.** We report success rates (S.R.) for standard single-arm and dual-arm tasks (left), and a long-horizon task evaluated over three consecutive steps (right).

Models	Wipe	Press	Place dish	Place egg	Scoop popcorn	Open pot	Mean	Place egg on bread (Long-horizon)				
	blackboard	stamp	on rack	on bread	into bowl	pick corn	S.R. ↑	Step 1	→	Step 2	→	Step 3
SpatialVLA [64]	0.60	0.67	0.30	0.20	0.27	0.40	0.39	0.20		0.07		0.00
$\pi_{0.5}$ [35]	0.60	0.73	0.60	0.47	0.53	0.60	0.59	0.47		0.20		0.07
CoT-VLA [92]	0.53	0.60	0.66	0.53	0.33	0.53	0.53	0.33		0.13		0.07
LaST ₀	0.73	0.93	0.80	0.66	0.66	0.53	0.72	0.66		0.47		0.33

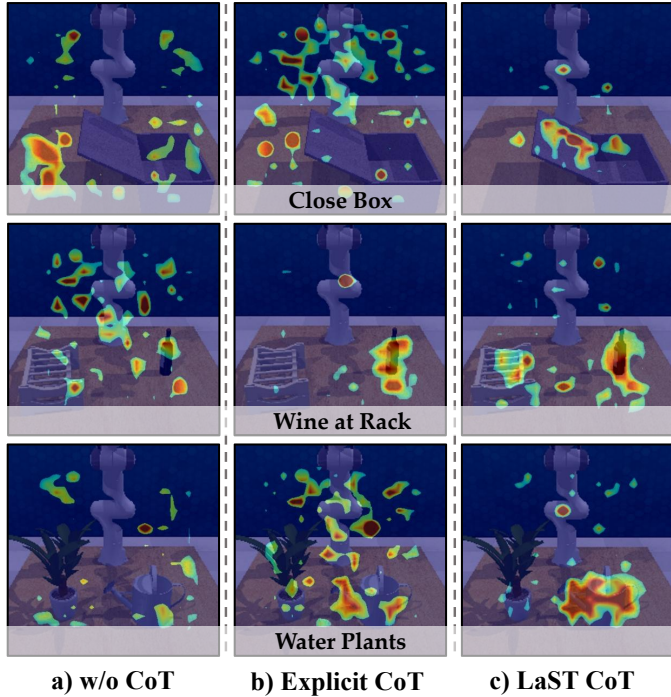


Fig. 5: Attention heatmap visualizations from the last layer for three VLA models: (a) LaST₀ without CoT reasoning, (b) the explicit CoT in CoT-VLA, and (c) LaST₀ with LaST CoT.

that each modality-specific latent provides a strong basis for action generation. The combination of multiple modality latents continues to provide additional performance improvements, even when the manipulation accuracy is already high. These results validate the importance of modeling comprehensive physical dynamics in the latent space, and further demonstrate that enabling the model to autonomously reason about the relationship between the robot and its interactive environment is effective for robotic manipulation.

Number of tokens per latent modality. As shown in Fig. 4 b), we study how the token budget allocated to each latent modality affects performance by varying the number of latent tokens while keeping other components fixed. When no latent token is used, performance drops substantially to 68%, indicating that the absence of latent representations severely limits the model’s reasoning capacity. Introducing a single token for each modality leads to a sharp improvement (up to 82%), demonstrating that even a minimal latent representation is sufficient to establish an effective latent decision state.

Further increasing the number of tokens yields no signifi-

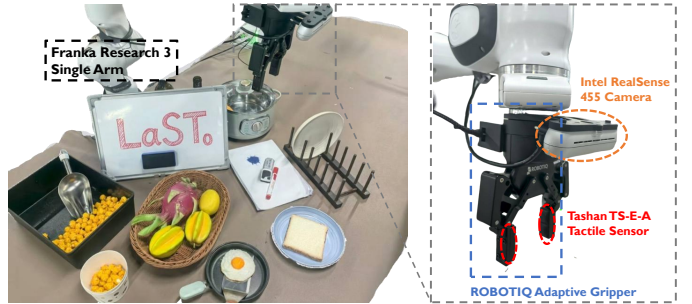


Fig. 6: Real-world Experiment Setup. We show the details about robot-arm setup and assets of manipulation tasks.

cant accuracy improvement, suggesting that high-level latent tokens can compactly encode physical information sufficient for effective reasoning.

Temporal coverage in latent reasoning. As shown in Fig. 4 c), we investigate the effect of the temporal horizon used in latent reasoning by varying the number of future time steps encoded into the latent state. Performance improves consistently as the latent temporal coverage increases (from 68% to 82% when extending from 0 to 4 steps), indicating that incorporating longer temporal dependencies enables more informed latent decision states. At the same time, expanding the temporal horizon introduces higher inference latency, revealing a trade-off between decision quality and computational efficiency in reasoning expert. Due to our fast–slow system design, extending the temporal horizon of the latent space does not significantly affect action generation speed.

Collaboration frequency between reasoning and action experts. As shown in Fig. 4 d), varying the collaboration frequency has a clear impact on task success. Fixed ratios such as 1:1, 1:2, and 1:4 achieve comparable performance (75–79%), while overly infrequent collaboration (1:8) leads to a relative drop to 74%. Finally, the mixed strategy trained by combining data from all four collaboration ratios achieves the best performance (82%), using a 1:4 ratio during testing. These results indicate that our frequency joint training scheme enables more robust coordination between the reasoning and action experts across tasks.

C. Real-World Experiment

Data collection. We evaluated our method on a set of real-world manipulation tasks using both single-arm and dual-arm Franka robot setups. As shown in Fig. 6, the single-arm platform consists of a Franka robot equipped with two Intel RealSense D455 cameras, providing third-person and wrist-

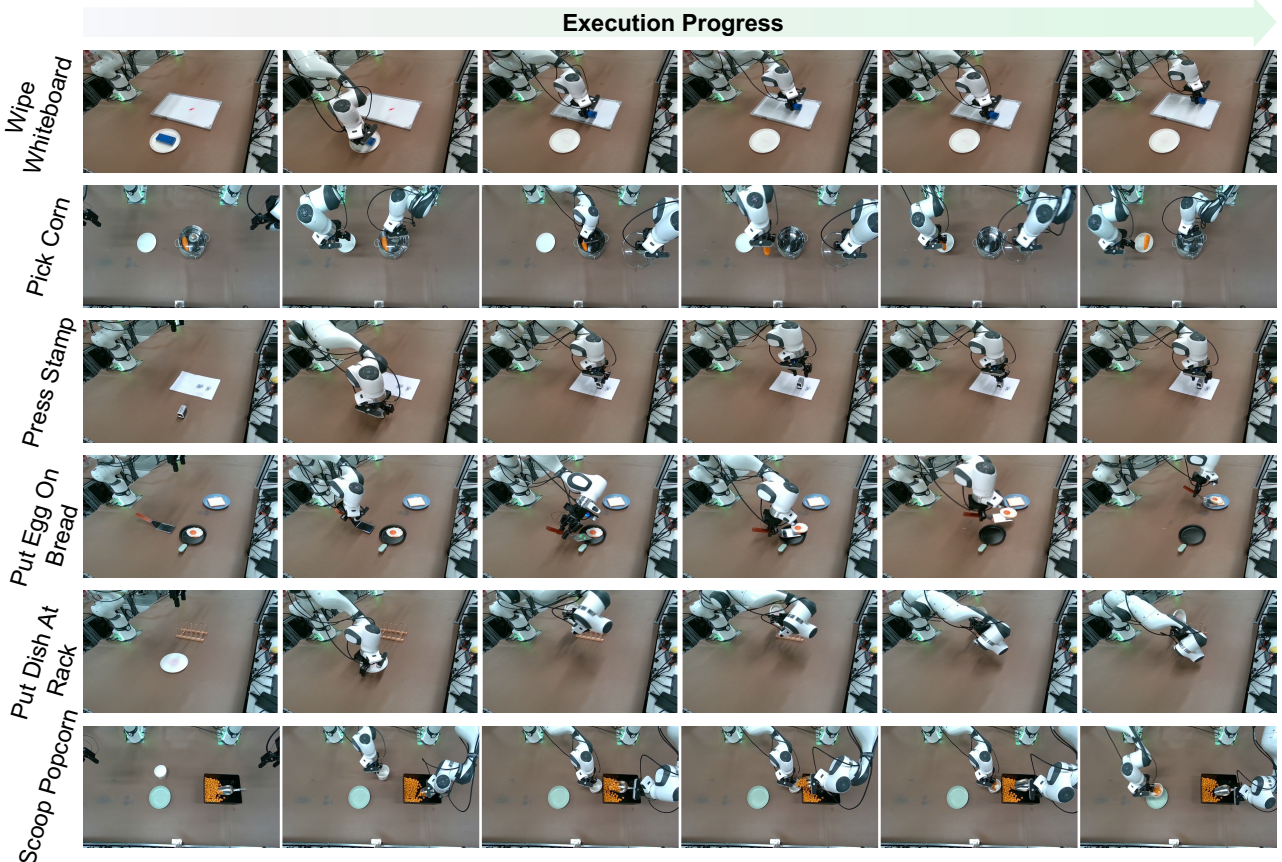


Fig. 7: Visualization of task execution processes by real-world single-arm and dual-arm robots (from left to right).

view RGB-D observations. The dual-arm setup combines two Franka robots and three D455 cameras, including one third-person view and two wrist-mounted views. In the single-arm setting, we collect demonstrations for three tasks: 1) *wiping a whiteboard with an eraser*, 2) *placing a dish on a rack*, and 3) *placing an egg on bread using a spatula*, which is a complex task requiring the robot to precisely scoop the egg and place it back onto the bread. In addition, we further evaluate a long-horizon setting on *placing egg* task, where the robot consecutively completes the full task three times while the positions of the manipulated objects continuously change during execution. For the dual-arm setting, two collaborative tasks were considered: 1) *scooping popcorn into a bowl* and 2) *opening a pot lid followed by picking corn from the pot*. All demonstrations were collected using the Gello platform [83], with 200 high-quality demonstrations per task. More details are provided in Appendix B and Appendix C.

Training and evaluation details. We train the LaST_0 policy following the same protocol as in simulation, with the only difference being the use of multi-view visual inputs in real-world settings: two camera views for the single-arm setup and three views for the dual-arm setup. We compare our method against three strong baselines: $\pi_{0.5}$ [5], a SOTA 2D VLA model; SpatialVLA [64], a SOTA 3D VLA model; and CoT-VLA [92], an explicit CoT-based VLA model that enhances

action generation by predicting future visual observations. For fair comparison, all models use the same number of camera viewpoints, and each task is evaluated with 15 rollouts under identical test conditions.

Quantitative and qualitative analysis. As shown in Table II, LaST_0 achieves the best overall performance on real-world manipulation tasks, with a mean success rate of 72%, substantially outperforming SpatialVLA (39%), $\pi_{0.5}$ (59%), and CoT-VLA (53%). LaST_0 consistently delivers strong gains across a diverse set of tasks, particularly those requiring precise spatial reasoning and temporally coherent control. For instance, on *Place dish on rack*, LaST_0 reaches a success rate of 80%, compared to 66% for CoT-VLA and 60% for $\pi_{0.5}$. On *Press stamp*, LaST_0 further achieves a success rate of 93%, significantly outperforming $\pi_{0.5}$ (73%) and CoT-VLA (60%). These results highlight the advantage of LaST_0 's latent spatio-temporal reasoning in modeling physical dynamics and robot-environment interactions in real-world settings.

We further evaluate LaST_0 on a long-horizon manipulation task that requires one, two, and three consecutive successful executions within a single rollout. As shown in Table II, LaST_0 maintains markedly higher success rates across all stages ($0.66 \rightarrow 0.47 \rightarrow 0.33$) compared to $\pi_{0.5}$ ($0.47 \rightarrow 0.20 \rightarrow 0.07$), with the performance gap widening as the horizon increases. Notably, at the third step, LaST_0 achieves nearly

a $5 \times$ higher success rate than $\pi_{0.5}$. This trend indicates that LaST₀ is better able to preserve coherent latent representations of task progress and environment state over extended horizons, enabling stable action generation.

Fig. 7 illustrates representative task executions across single-arm and dual-arm settings. We observe that LaST₀ produces smooth and continuous motions, particularly in precise actions such as surface wiping, spatula-mediated placement, and bimanual scooping. This behavior is enabled by the proposed LaST CoT and dual-system design, where a low-frequency reasoning expert provides temporally coherent latent guidance, while the action expert operates at a higher control frequency, allowing rapid and fine-grained response to environment dynamics. We also verify the model’s closed-loop capability: for example, when new marks are continuously drawn on the blackboard during manipulation, the robotic arm can persistently perform the erasing action.

V. CONCLUSION AND FUTURE WORK

In this work, we introduced LaST₀, a dual-system VLA model that enables efficient reason-before-act behavior for robotic manipulation through a Latent Spatio-Temporal Chain-of-Thought (LaST CoT). By shifting reasoning from explicit traces to a compact latent space, LaST₀ overcomes the latency and representational bottlenecks inherent in prior explicit CoT VLA approaches, while preserving the ability to model fine-grained physical dynamics essential for closed-loop control. Central to our framework is a token-efficient spatio-temporal latent representation that autoregressively captures future semantic, geometric, and proprioceptive dynamics. This design allows the model to form temporally coherent internal reasoning trajectories, bridging high-level intent understanding with low-level execution. Building upon this LaST CoT mechanism, we further proposed a fast–slow dual-system architecture implemented via a Mixture-of-Transformers, which decouples low-frequency deliberative reasoning from high-frequency action generation. The resulting asynchronous coordination enables real-time responsiveness without sacrificing CoT reasoning capability. We believe LaST₀ represents a step toward more scalable and physically grounded reasoning in robotic foundation models.

Future work will further explore richer designs of the latent spatio-temporal reasoning space, enabling more expressive and structured physical abstractions. We also plan to investigate advanced post-training strategies, such as jointly optimizing latent reasoning and action generation via reinforcement learning, as well as scaling LaST₀ to more complex long-horizon manipulation tasks with delayed rewards, contact-rich dynamics, and evolving environments.

ACKNOWLEDGMENTS

REFERENCES

- [1] Jean-Baptiste Alayrac, Jeff Donahue, Pauline Luc, Antoine Miech, Iain Barr, Yana Hasson, Karel Lenc, Arthur Mensch, Katherine Millican, Malcolm Reynolds, et al. Flamingo: a visual language model for few-shot learning. *Advances in Neural Information Processing Systems*, 35: 23716–23736, 2022.
- [2] Suneel Belkhale, Yuchen Cui, and Dorsa Sadigh. Hydra: Hybrid robot actions for imitation learning. *arxiv*, 2023.
- [3] Suneel Belkhale, Tianli Ding, Ted Xiao, Pierre Sermanet, Quon Vuong, Jonathan Tompson, Yevgen Chebotar, Debiddatta Dwibedi, and Dorsa Sadigh. Rt-h: Action hierarchies using language, 2024. URL <https://arxiv.org/abs/2403.01823>.
- [4] Johan Bjorck, Fernando Castañeda, Nikita Cherniadev, Xingye Da, Runyu Ding, Linxi Fan, Yu Fang, Dieter Fox, Fengyuan Hu, Spencer Huang, et al. Gr0ot n1: An open foundation model for generalist humanoid robots. *arXiv preprint arXiv:2503.14734*, 2025.
- [5] Kevin Black, Noah Brown, Danny Driess, Adnan Esmail, Michael Equi, Chelsea Finn, Niccolò Fusai, Lachy Groom, Karol Hausman, Brian Ichter, et al. pi0: A vision-language-action flow model for general robot control. *arXiv preprint arXiv:2410.24164*, 2024.
- [6] Anthony Brohan, Noah Brown, Justice Carbajal, Yevgen Chebotar, Joseph Dabis, Chelsea Finn, Keerthana Gopalakrishnan, Karol Hausman, Alex Herzog, Jasmine Hsu, Julian Ibarz, et al. Rt-1: Robotics transformer for real-world control at scale. In *arXiv preprint arXiv:2212.06817*, 2022.
- [7] Anthony Brohan, Noah Brown, Justice Carbajal, Yevgen Chebotar, Xi Chen, Krzysztof Choromanski, Tianli Ding, Danny Driess, Avinava Dubey, Chelsea Finn, et al. Rt-2: Vision-language-action models transfer web knowledge to robotic control. In *arXiv preprint arXiv:2307.15818*, 2023.
- [8] Qingwen Bu, Jisong Cai, Li Chen, Xiuqi Cui, Yan Ding, Siyuan Feng, Shenyuan Gao, Xindong He, Xuan Hu, Xu Huang, et al. Agibot world colosseo: A large-scale manipulation platform for scalable and intelligent embodied systems. *arXiv preprint arXiv:2503.06669*, 2025.
- [9] Jun Cen, Chaohui Yu, Hangjie Yuan, Yuming Jiang, Siteng Huang, Jiayan Guo, Xin Li, Yibing Song, Hao Luo, Fan Wang, et al. Worldvla: Towards autoregressive action world model. *arXiv preprint arXiv:2506.21539*, 2025.
- [10] Jiayi Chen, Wenxuan Song, Pengxiang Ding, Ziyang Zhou, Han Zhao, Feilong Tang, Donglin Wang, and Haoang Li. Unified diffusion vla: Vision-language-action model via joint discrete denoising diffusion process, 2025. URL <https://arxiv.org/abs/2511.01718>.
- [11] Lawrence Yunliang Chen, Simeon Adebola, and Ken Goldberg. Berkeley UR5 demonstration dataset. <https://sites.google.com/view/berkeley-ur5/home>.
- [12] Xiaokang Chen, Zhiyu Wu, Xingchao Liu, Zizheng Pan, Wen Liu, Zhenda Xie, Xingkai Yu, and Chong Ruan. Janus-pro: Unified multimodal understanding and generation with data and model scaling. *arXiv preprint arXiv:2501.17811*, 2025.
- [13] Xinghao Chen, Anhao Zhao, Heming Xia, Xuan Lu,

Hanlin Wang, Yanjun Chen, Wei Zhang, Jian Wang, Wanjie Li, and Xiaoyu Shen. Reasoning beyond language: A comprehensive survey on latent chain-of-thought reasoning. *arXiv preprint arXiv:2505.16782*, 2025.

[14] Yuhui Chen, Shuai Tian, Shugao Liu, Yingting Zhou, Haoran Li, and Dongbin Zhao. Conrft: A reinforced fine-tuning method for vla models via consistency policy. *arXiv preprint arXiv:2502.05450*, 2025.

[15] Zengjue Chen, Runliang Niu, He Kong, Qi Wang, Qianli Xing, and Zipei Fan. Tgrpo :fine-tuning vision-language-action model via trajectory-wise group relative policy optimization, 2025. URL <https://arxiv.org/abs/2506.08440>.

[16] Cheng Chi, Siyuan Feng, Yilun Du, Zhenjia Xu, Eric Cousineau, Benjamin Burchfiel, and Shuran Song. Diffusion policy: Visuomotor policy learning via action diffusion. In *Proceedings of Robotics: Science and Systems (RSS)*, 2023.

[17] Zichen Jeff Cui, Yibin Wang, Nur Muhammad Mahi Shafiuallah, and Lerrel Pinto. From play to policy: Conditional behavior generation from uncurated robot data. *arXiv preprint arXiv:2210.10047*, 2022.

[18] Sudeep Dasari, Frederik Ebert, Stephen Tian, Suraj Nair, Bernadette Bucher, Karl Schmeckpeper, Siddharth Singh, Sergey Levine, and Chelsea Finn. Robonet: Large-scale multi-robot learning. In *Conference on Robot Learning*, pages 885–897. PMLR, 2020.

[19] Shivin Dass, Julian Yapeter, Jesse Zhang, Jiahui Zhang, Karl Pertsch, Stefanos Nikolaidis, and Joseph J. Lim. CLVR jaco play dataset, 2023. URL https://github.com/clvrai/clvr_jaco_play_dataset.

[20] Chaorui Deng, Deyao Zhu, Kunchang Li, Chenhui Gou, Feng Li, Zeyu Wang, Shu Zhong, Weihao Yu, Xiaonan Nie, Ziang Song, Guang Shi, and Haoqi Fan. Emerging properties in unified multimodal pretraining, 2025. URL <https://arxiv.org/abs/2505.14683>.

[21] Chaorui Deng, Deyao Zhu, Kunchang Li, Chenhui Gou, Feng Li, Zeyu Wang, Shu Zhong, Weihao Yu, Xiaonan Nie, Ziang Song, et al. Emerging properties in unified multimodal pretraining. *arXiv preprint arXiv:2505.14683*, 2025.

[22] Shengliang Deng, Mi Yan, Songlin Wei, Haixin Ma, Yuxin Yang, Jiayi Chen, Zhiqi Zhang, Taoyu Yang, Xuheng Zhang, Wenhao Zhang, et al. Graspvla: a grasping foundation model pre-trained on billion-scale synthetic action data. *arXiv preprint arXiv:2505.03233*, 2025.

[23] Yuntian Deng, Yejin Choi, and Stuart Shieber. From explicit cot to implicit cot: Learning to internalize cot step by step. *arXiv preprint arXiv:2405.14838*, 2024.

[24] Frederik Ebert, Yanlai Yang, Karl Schmeckpeper, Bernadette Bucher, Georgios Georgakis, Kostas Daniilidis, Chelsea Finn, and Sergey Levine. Bridge data: Boosting generalization of robotic skills with cross-domain datasets. In *RSS*, 2022.

[25] Zipeng Fu, Tony Z Zhao, and Chelsea Finn. Mobile aloha: Learning bimanual mobile manipulation with low-cost whole-body teleoperation. *arXiv preprint arXiv:2401.02117*, 2024.

[26] Shenyuan Gao, Siyuan Zhou, Yilun Du, Jun Zhang, and Chuang Gan. Adaworld: Learning adaptable world models with latent actions. *arXiv preprint arXiv:2503.18938*, 2025.

[27] Ankit Goyal, Jie Xu, Yijie Guo, Valts Blukis, Yu-Wei Chao, and Dieter Fox. Rvt: Robotic view transformer for 3d object manipulation. In *Conference on Robot Learning*, pages 694–710. PMLR, 2023.

[28] Chenyang Gu, Jiaming Liu, Hao Chen, Runzhong Huang, Qingpo Wuwu, Zhuoyang Liu, Xiaoqi Li, Ying Li, Renrui Zhang, Peng Jia, et al. Manualvla: A unified vla model for chain-of-thought manual generation and robotic manipulation. *arXiv preprint arXiv:2512.02013*, 2025.

[29] Jiayuan Gu, Fanbo Xiang, Xuanlin Li, Zhan Ling, Xiqiang Liu, Tongzhou Mu, Yihe Tang, Stone Tao, Xinyue Wei, Yunchao Yao, Xiaodi Yuan, Pengwei Xie, Zhiao Huang, Rui Chen, and Hao Su. Maniskill2: A unified benchmark for generalizable manipulation skills, 2023. URL <https://arxiv.org/abs/2302.04659>.

[30] Daya Guo, Dejian Yang, Haowei Zhang, Junxiao Song, Ruoyu Zhang, Runxin Xu, Qihao Zhu, Shirong Ma, Peiyi Wang, Xiao Bi, et al. Deepseek-r1: Incentivizing reasoning capability in llms via reinforcement learning. *arXiv preprint arXiv:2501.12948*, 2025.

[31] Shibo Hao, Sainbayar Sukhbaatar, DiJia Su, Xian Li, Zhiting Hu, Jason Weston, and Yuandong Tian. Training large language models to reason in a continuous latent space. *arXiv preprint arXiv:2412.06769*, 2024.

[32] Minho Heo, Youngwoon Lee, Doohyun Lee, and Joseph J. Lim. Furniturebench: Reproducible real-world benchmark for long-horizon complex manipulation. In *Robotics: Science and Systems*, 2023.

[33] Chengkai Hou, Kun Wu, Jiaming Liu, Zhengping Che, Di Wu, Fei Liao, Guangrun Li, Jingyang He, Qiuxuan Feng, Zhao Jin, et al. Robomind 2.0: A multimodal, bimanual mobile manipulation dataset for generalizable embodied intelligence. *arXiv preprint arXiv:2512.24653*, 2025.

[34] Chi-Pin Huang, Yueh-Hua Wu, Min-Hung Chen, Yu-Chiang Frank Wang, and Fu-En Yang. Thinkact: Vision-language-action reasoning via reinforced visual latent planning. *arXiv preprint arXiv:2507.16815*, 2025.

[35] Physical Intelligence, Kevin Black, Noah Brown, James Darpinian, Karan Dhabalia, Danny Driess, Adnan Esmail, Michael Equi, Chelsea Finn, et al. $\pi_{0.5}$: a vision-language-action model with open-world generalization, 2025. URL <https://arxiv.org/abs/2504.16054>.

[36] Stephen James, Zicong Ma, David Rovick Arrojo, and Andrew J Davison. Rlbench: The robot learning benchmark & learning environment. *IEEE Robotics and Automation Letters*, 5(2):3019–3026, 2020.

[37] Eric Jang, Alex Irpan, Mohi Khansari, Daniel Kappler, Frederik Ebert, Corey Lynch, Sergey Levine, and Chelsea

Finn. Bc-z: Zero-shot task generalization with robotic imitation learning. In *Conference on Robot Learning*, pages 991–1002. PMLR, 2022.

[38] Yueru Jia, Jiaming Liu, Sixiang Chen, Chenyang Gu, Zhilue Wang, Longzan Luo, Lily Lee, Pengwei Wang, Zhongyuan Wang, Renrui Zhang, et al. Lift3d foundation policy: Lifting 2d large-scale pretrained models for robust 3d robotic manipulation. *arXiv preprint arXiv:2411.18623*, 2024.

[39] Dmitry Kalashnikov, Alex Irpan, Peter Pastor, Julian Ibarz, Alexander Herzog, Eric Jang, Deirdre Quillen, Ethan Holly, Mrinal Kalakrishnan, Vincent Vanhoucke, et al. QT-Opt: Scalable deep reinforcement learning for vision-based robotic manipulation. *arXiv preprint arXiv:1806.10293*, 2018.

[40] Siddharth Karamcheti, Suraj Nair, Ashwin Balakrishna, Percy Liang, Thomas Kollar, and Dorsa Sadigh. Prismatic vlms: Investigating the design space of visually-conditioned language models. In *Forty-first International Conference on Machine Learning*, 2024.

[41] Alexander Khazatsky, Karl Pertsch, Suraj Nair, Ashwin Balakrishna, Sudeep Dasari, Siddharth Karamcheti, Soroush Nasiriany, Mohan Kumar Srirama, Lawrence Yunliang Chen, Kirsty Ellis, Peter David Fagan, Joey Hejna, Masha Itkina, Marion Lepert, Yecheng Jason Ma, Patrick Tree Miller, Jimmy Wu, Suneel Belkhale, Shivin Dass, Huy Ha, Arhan Jain, Abraham Lee, Youngwoon Lee, Marius Memmel, Sungjae Park, Ilija Radosavovic, Kaiyuan Wang, Albert Zhan, Kevin Black, Cheng Chi, Kyle Beltran Hatch, Shan Lin, Jingpei Lu, Jean Mercat, Abdul Rehman, Pannag R Sanketi, Archit Sharma, Cody Simpson, Quan Vuong, Homer Rich Walke, Blake Wulfe, Ted Xiao, Jonathan Heewon Yang, Arefeh Yavary, Tony Z. Zhao, Christopher Agia, Rohan Baijal, Mateo Guaman Castro, Daphne Chen, Qiuyu Chen, Trinity Chung, Jaimyn Drake, Ethan Paul Foster, Jensen Gao, David Antonio Herrera, Minho Heo, Kyle Hsu, Jiaheng Hu, Donovon Jackson, Charlotte Le, Yunshuang Li, Kevin Lin, Roy Lin, Zehan Ma, Abhiram Maddukuri, Suvir Mirchandani, Daniel Morton, Tony Nguyen, Abigail O'Neill, Rosario Scalise, Derick Seale, Victor Son, Stephen Tian, Emi Tran, Andrew E. Wang, Yilin Wu, Annie Xie, Jingyun Yang, Patrick Yin, Yunchu Zhang, Osbert Bastani, Glen Berseth, Jeannette Bohg, Ken Goldberg, Abhinav Gupta, Abhishek Gupta, Dinesh Jayaraman, Joseph J Lim, Jitendra Malik, Roberto Martín-Martín, Subramanian Ramamoorthy, Dorsa Sadigh, Shuran Song, Jiajun Wu, Michael C. Yip, Yuke Zhu, Thomas Kollar, Sergey Levine, and Chelsea Finn. Droid: A large-scale in-the-wild robot manipulation dataset. 2024.

[42] Moo Jin Kim, Karl Pertsch, Siddharth Karamcheti, Ted Xiao, Ashwin Balakrishna, Suraj Nair, Rafael Rafailov, Ethan Foster, Grace Lam, Pannag Sanketi, et al. Openvla: An open-source vision-language-action model. *arXiv preprint arXiv:2406.09246*, 2024.

[43] Vikash Kumar, Rutav Shah, Gaoyue Zhou, Vincent Moens, Vittorio Caggiano, Abhishek Gupta, and Aravind Rajeswaran. Robohive: A unified framework for robot learning. In *Thirty-seventh Conference on Neural Information Processing Systems Datasets and Benchmarks Track*, 2023.

[44] Haozhan Li, Yuxin Zuo, Jiale Yu, Yuhao Zhang, Zhao-hui Yang, Kaiyan Zhang, Xuekai Zhu, Yuchen Zhang, Tianxing Chen, Ganqu Cui, Dehui Wang, Dingxiang Luo, Yuchen Fan, Youbang Sun, Jia Zeng, Jiangmiao Pang, Shanghang Zhang, Yu Wang, Yao Mu, Bowen Zhou, and Ning Ding. Simplevla-rl: Scaling vla training via reinforcement learning, 2025. URL <https://arxiv.org/abs/2509.09674>.

[45] Jinming Li, Yichen Zhu, Zhibin Tang, Junjie Wen, Minjie Zhu, Xiaoyu Liu, Chengmeng Li, Ran Cheng, Yixin Peng, and Feifei Feng. Improving vision-language-action models via chain-of-affordance. *arXiv preprint arXiv:2412.20451*, 2024.

[46] Jinming Li, Yichen Zhu, Zhibin Tang, Junjie Wen, Minjie Zhu, Xiaoyu Liu, Chengmeng Li, Ran Cheng, Yixin Peng, Yan Peng, et al. Coa-vla: Improving vision-language-action models via visual-text chain-of-affordance. In *Proceedings of the IEEE/CVF International Conference on Computer Vision*, pages 9759–9769, 2025.

[47] Qixiu Li, Yaobo Liang, Zeyu Wang, Lin Luo, Xi Chen, Mozheng Liao, Fangyun Wei, Yu Deng, Sicheng Xu, Yizhong Zhang, et al. Cogact: A foundational vision-language-action model for synergizing cognition and action in robotic manipulation. *arXiv preprint arXiv:2411.19650*, 2024.

[48] Xiaoqi Li, Mingxu Zhang, Yiran Geng, Haoran Geng, Yuxing Long, Yan Shen, Renrui Zhang, Jiaming Liu, and Hao Dong. Manipllm: Embodied multimodal large language model for object-centric robotic manipulation, 2023. URL <https://arxiv.org/abs/2312.16217>.

[49] Fanqi Lin, Ruiqian Nai, Yingdong Hu, Jiacheng You, Junming Zhao, and Yang Gao. Onetwovla: A unified vision-language-action model with adaptive reasoning. *arXiv preprint arXiv:2505.11917*, 2025.

[50] Jiaming Liu, Hao Chen, Pengju An, Zhuoyang Liu, Renrui Zhang, Chenyang Gu, Xiaoqi Li, Ziyu Guo, Sixiang Chen, Mengzhen Liu, et al. Hybridvla: Collaborative diffusion and autoregression in a unified vision-language-action model. *arXiv preprint arXiv:2503.10631*, 2025.

[51] Songming Liu, Lingxuan Wu, Bangguo Li, Hengkai Tan, Huayu Chen, Zhengyi Wang, Ke Xu, et al. Rdt-1b: a diffusion foundation model for bimanual manipulation. In *The Thirteenth International Conference on Learning Representations*.

[52] Zhuoyang Liu, Jiaming Liu, Jiadong Xu, Nuowei Han, Chenyang Gu, Hao Chen, Kaichen Zhou, Renrui Zhang, Kai Chin Hsieh, Kun Wu, et al. Mla: A multisensory language-action model for multimodal understanding and forecasting in robotic manipulation. *arXiv preprint*

arXiv:2509.26642, 2025.

[53] Ilya Loshchilov and Frank Hutter. Decoupled weight decay regularization. *arXiv preprint arXiv:1711.05101*, 2017.

[54] Guanxing Lu, Wenkai Guo, Chubin Zhang, Yuheng Zhou, Haonan Jiang, Zifeng Gao, Yansong Tang, and Ziwei Wang. Vla-rl: Towards masterful and general robotic manipulation with scalable reinforcement learning. *arXiv preprint arXiv:2505.18719*, 2025.

[55] Jianlan Luo, Charles Xu, Fangchen Liu, Liam Tan, Zipeng Lin, Jeffrey Wu, Pieter Abbeel, and Sergey Levine. FMB: A functional manipulation benchmark for generalizable robotic learning. <https://functional-manipulation-benchmark.github.io>, 2023.

[56] Corey Lynch, Ayzaan Wahid, Jonathan Tompson, Tianli Ding, James Betker, Robert Baruch, Travis Armstrong, and Pete Florence. Interactive language: Talking to robots in real time. *IEEE Robotics and Automation Letters*, 2023.

[57] Ajay Mandlekar, Yuke Zhu, Animesh Garg, Jonathan Booher, Max Spero, Albert Tung, Julian Gao, John Emmons, Anchit Gupta, Emre Orbay, Silvio Savarese, and Li Fei-Fei. RoboTurk: A crowdsourcing platform for robotic skill learning through imitation. *CoRR*, abs/1811.02790, 2018.

[58] Tatsuya Matsushima, Hiroki Furuta, Yusuke Iwasawa, and Yutaka Matsuo. Weblab xarm dataset, 2023.

[59] Oier Mees, Jessica Borja-Diaz, and Wolfram Burgard. Grounding language with visual affordances over unstructured data. In *Proceedings of the IEEE International Conference on Robotics and Automation (ICRA)*, London, UK, 2023.

[60] Russell Mendonca, Shikhar Bahl, and Deepak Pathak. Structured world models from human videos. *CoRL*, 2023.

[61] Jihoon Oh, Naoaki Kanazawa, and Kento Kawaharazuka. X-embodiment u-tokyo pr2 datasets, 2023. URL https://github.com/ojh6404/rlds_dataset_builder.

[62] Open X-Embodiment Collaboration, Abhishek Padalkar, Acorn Pooley, et al. Open X-Embodiment: Robotic learning datasets and RT-X models. <https://arxiv.org/abs/2310.08864>, 2023.

[63] Abhishek Padalkar, Gabriel Quere, Antonin Raffin, João Silvério, and Freek Stulp. A guided reinforcement learning approach using shared control templates for learning manipulation skills in the real world. 2023.

[64] Delin Qu, Haoming Song, Qizhi Chen, Yuanqi Yao, Xinyi Ye, Yan Ding, Zhigang Wang, JiaYuan Gu, et al. Spatialvla: Exploring spatial representations for visual-language-action model. *arXiv preprint arXiv:2501.15830*, 2025.

[65] Erick Rosete-Beas, Oier Mees, Gabriel Kalweit, Joschka Boedecker, and Wolfram Burgard. Latent plans for task agnostic offline reinforcement learning. In *Proceedings of the 6th Conference on Robot Learning (CoRL)*, 2022.

[66] Nur Muhammad Mahi Shafiullah, Anant Rai, Haritheja Etukuru, Yiqian Liu, Ishan Misra, Soumith Chintala, and Lerrel Pinto. On bringing robots home, 2023.

[67] Mohit Shridhar, Lucas Manuelli, and Dieter Fox. Perceiver-actor: A multi-task transformer for robotic manipulation. In *Proceedings of the 6th Conference on Robot Learning (CoRL)*, 2022.

[68] Ioan A Sucan, Mark Moll, and Lydia E Kavraki. The open motion planning library. *IEEE Robotics & Automation Magazine*, 19(4):72–82, 2012.

[69] Shuhan Tan, Kashyap Chitta, Yuxiao Chen, Ran Tian, Yurong You, Yan Wang, Wenjie Luo, Yulong Cao, Philipp Krahenbuhl, Marco Pavone, et al. Latent chain-of-thought world modeling for end-to-end driving. *arXiv preprint arXiv:2512.10226*, 2025.

[70] Shuhan Tan, Kairan Dou, Yue Zhao, and Philipp Krähenbühl. Interactive post-training for vision-language-action models, 2025. URL <https://arxiv.org/abs/2505.17016>.

[71] Yang Tian, Sizhe Yang, Jia Zeng, Ping Wang, Dahua Lin, Hao Dong, and Jiangmiao Pang. Predictive inverse dynamics models are scalable learners for robotic manipulation, 2024. URL <https://arxiv.org/abs/2412.15109>.

[72] Faraz Torabi, Garrett Warnell, and Peter Stone. Behavioral cloning from observation. *arXiv preprint arXiv:1805.01954*, 2018.

[73] Homer Walke, Kevin Black, Abraham Lee, Moo Jin Kim, Max Du, Chongyi Zheng, Tony Zhao, Philippe Hansen-Estruch, Quan Vuong, Andre He, Vivek Myers, Kuan Fang, Chelsea Finn, and Sergey Levine. Bridgedata v2: A dataset for robot learning at scale, 2023.

[74] Jianyuan Wang, Minghao Chen, Nikita Karaev, Andrea Vedaldi, Christian Rupprecht, and David Novotny. Vggt: Visual geometry grounded transformer. In *Proceedings of the Computer Vision and Pattern Recognition Conference*, pages 5294–5306, 2025.

[75] Peng Wang, Shuai Bai, Sinan Tan, Shijie Wang, Zhihao Fan, Jinze Bai, Keqin Chen, Xuejing Liu, Jialin Wang, Wenbin Ge, et al. Qwen2-vl: Enhancing vision-language model’s perception of the world at any resolution. *arXiv preprint arXiv:2409.12191*, 2024.

[76] Qixun Wang, Yang Shi, Yifei Wang, Yuanxing Zhang, Pengfei Wan, Kun Gai, Xianghua Ying, and Yisen Wang. Monet: Reasoning in latent visual space beyond images and language. *arXiv preprint arXiv:2511.21395*, 2025.

[77] Yuqi Wang, Xinghang Li, Wenxuan Wang, Junbo Zhang, Yingyan Li, Yuntao Chen, Xinlong Wang, and Zhaoxiang Zhang. Unified vision-language-action model. *arXiv preprint arXiv:2506.19850*, 2025.

[78] Yuqi Wang, Xinghang Li, Wenxuan Wang, Junbo Zhang, Yingyan Li, Yuntao Chen, Xinlong Wang, and Zhaoxiang Zhang. Unified vision-language-action model, 2025. URL <https://arxiv.org/abs/2506.19850>.

[79] Junjie Wen, Minjie Zhu, Yichen Zhu, Zhibin Tang, Jinming Li, Zhongyi Zhou, Chengmeng Li, Xiaoyu Liu, Yaxin Peng, Chaomin Shen, et al. Diffusion-vla: Scaling robot foundation models via unified diffusion and

autoregression. *arXiv preprint arXiv:2412.03293*, 2024.

[80] Junjie Wen, Yichen Zhu, Jinming Li, Zhibin Tang, Chaomin Shen, and Feifei Feng. Dexvla: Vision-language model with plug-in diffusion expert for general robot control. *arXiv preprint arXiv:2502.05855*, 2025.

[81] Junjie Wen, Yichen Zhu, Jinming Li, Minjie Zhu, Zhibin Tang, Kun Wu, Zhiyuan Xu, Ning Liu, Ran Cheng, Chaomin Shen, et al. Tinyvla: Towards fast, data-efficient vision-language-action models for robotic manipulation. *IEEE Robotics and Automation Letters*, 2025.

[82] Kun Wu, Chengkai Hou, Jiaming Liu, Zhengping Che, Xiaozhu Ju, et al. Robomind: Benchmark on multi-embodiment intelligence normative data for robot manipulation. In *Robotics: Science and Systems (RSS) 2025*. Robotics: Science and Systems Foundation, 2025.

[83] Philipp Wu, Yide Shentu, Zhongke Yi, Xingyu Lin, and Pieter Abbeel. Gello: A general, low-cost, and intuitive teleoperation framework for robot manipulators, 2024. URL <https://arxiv.org/abs/2309.13037>.

[84] Zeyuan Yang, Xueyang Yu, Delin Chen, Maohao Shen, and Chuang Gan. Machine mental imagery: Empower multimodal reasoning with latent visual tokens. *arXiv preprint arXiv:2506.17218*, 2025.

[85] Angen Ye, Zeyu Zhang, Boyuan Wang, Xiaofeng Wang, Dapeng Zhang, and Zheng Zhu. Vla-r1: Enhancing reasoning in vision-language-action models. *arXiv preprint arXiv:2510.01623*, 2025.

[86] Michał Zawalski, William Chen, Karl Pertsch, Oier Mees, Chelsea Finn, and Sergey Levine. Robotic control via embodied chain-of-thought reasoning, 2025. URL <https://arxiv.org/abs/2407.08693>.

[87] Xiaohua Zhai, Basil Mustafa, Alexander Kolesnikov, and Lucas Beyer. Sigmoid loss for language image pre-training. In *International Conference on Computer Vision (ICCV)*, 2023.

[88] Jianke Zhang, Yanjiang Guo, Yucheng Hu, Xiaoyu Chen, Xiang Zhu, and Jianyu Chen. Up-vla: A unified understanding and prediction model for embodied agent. *arXiv preprint arXiv:2501.18867*, 2025.

[89] Renrui Zhang, Xinyu Wei, Dongzhi Jiang, Ziyu Guo, Shicheng Li, Yichi Zhang, Chengzhuo Tong, Jiaming Liu, Aojun Zhou, Bin Wei, et al. Mavis: Mathematical visual instruction tuning with an automatic data engine. *arXiv preprint arXiv:2407.08739*, 2024.

[90] Wenyao Zhang, Hongsi Liu, Zekun Qi, Yunnan Wang, Xinqiang Yu, Jiazhao Zhang, Runpei Dong, Jiawei He, He Wang, Zhizheng Zhang, et al. Dreamvla: a vision-language-action model dreamed with comprehensive world knowledge. *arXiv preprint arXiv:2507.04447*, 2025.

[91] Zijian Zhang, Kaiyuan Zheng, Zhaorun Chen, Joel Jang, Yi Li, Siwei Han, Chaoqi Wang, Mingyu Ding, Dieter Fox, and Huaxiu Yao. Grape: Generalizing robot policy via preference alignment. *arXiv preprint arXiv:2411.19309*, 2024.

[92] Qingqing Zhao, Yao Lu, Moo Jin Kim, Zipeng Fu, Zhuoyang Zhang, Yecheng Wu, Zhaoshuo Li, Qianli Ma, Song Han, Chelsea Finn, et al. Cot-vla: Visual chain-of-thought reasoning for vision-language-action models. In *Proceedings of the Computer Vision and Pattern Recognition Conference*, pages 1702–1713, 2025.

[93] Gaoyue Zhou, Victoria Dean, Mohan Kumar Srirama, Aravind Rajeswaran, Jyothish Pari, Kyle Hatch, Aryan Jain, Tianhe Yu, Pieter Abbeel, Lerrel Pinto, Chelsea Finn, and Abhinav Gupta. Train offline, test online: A real robot learning benchmark, 2023.

[94] Junsheng Zhou, Jinsheng Wang, Baorui Ma, Yu-Shen Liu, Tiejun Huang, and Xinlong Wang. Uni3d: Exploring unified 3d representation at scale, 2023. URL <https://arxiv.org/abs/2310.06773>.

APPENDIX

A. Large Scale Pre-training Datasets

To ensure LaST₀ inherits a robust foundation of motor primitives and physical common sense, we curated a diverse corpus of 400K trajectories (28M frames) from the Open-X-Embodiment [62], DROID[41], and RoboMIND[82] repositories. Table III lists the detailed proportions of each dataset used. Specifically, to empower the slow reasoning expert with early geometric awareness, we utilized VGGT [74] to generate synthetic 3D point clouds for all pretraining frames. These generated point clouds serve as the initial 3D geometric latent (z^p) inputs within the LaST CoT, allowing the model to learn spatial occupancy and environment dynamics even in the absence of real-world depth sensors during pretraining. This strategic alignment ensures a seamless transition to the full multimodal laST CoT space during fine-tuning.

TABLE III: **Datasets used for pre-training.** The names of selected datasets for large-scale pretraining and their sampling ratios (%).

Dataset	Ratio (%)
BC-Z [37]	7.54
Berkeley Autolab Ur5 [11]	0.35
BridgeV2 [24, 73]	20.93
CMU Stretch [60]	0.02
DLR Sara Grid Clamp [63]	0.02
DROID [41]	4.82
Dobb-E [66]	0.18
FMB Dataset [55]	1.50
Fractal [6]	13.67
Furniture Bench [32]	0.09
Jaco Play [19]	0.19
Kuka [39]	20.22
Language Table [56]	7.72
Maniskill [29]	5.26
Nyu Franka Play [17]	0.24
Robo-Net [18]	11.53
Roboset [43]	3.21
RoboTurk [57]	0.70
Stanford Hydra [2]	0.20
Taco Play [65, 59]	1.26
Toto [93]	0.17
Utokyo Pr2 Fridge [61]	0.01
Utokyo Pr2 Tabletop [61]	0.04
Utokyo Xarm Pap [58]	0.04
RoboMIND [82]	0.2

B. Real-world Set-up

The physical deployment of LaST₀ utilizes a modular robotic infrastructure designed to provide the rich multi-modal feedback necessary for deliberative reasoning and responsive control. As shown in Fig. 6, for single-arm configurations, we deploy a Franka Research 3 (FR3) manipulator paired with a ROBOTIQ adaptive gripper. The perceptual backbone consists of two Intel RealSense D455 cameras: a stationary third-person unit providing the right-front perspective required

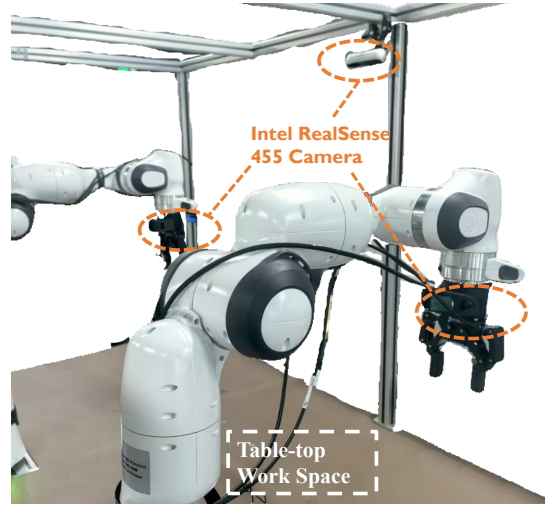


Fig. 8: Dual-arm Setup. We show the details about dual-arm setup, including robot arms and cameras.

for the Slow Reasoning Expert's spatio-temporal planning, and a wrist-mounted unit for high-frequency visual servoing. To ground the Latent CoT in physical contact dynamics, we integrate dual Tashan TS-E-A tactile sensors into the gripper fingertips.

As shown in Fig. 8, in dual-arm scenarios, the architecture scales to two parallel FR3 arms with identical end-effector and haptic configurations. This bimanual setup expands the perceptual suite to a three-camera array, including an additional front view camera and dual wrist cameras to capture the complex, synchronized spatio-temporal dependencies essential for collaborative manipulation.

C. Self Collected Data

Building upon our real-world experiment setup, we evaluate LaST₀ across six representative tasks. These scenarios are specifically designed to validate the model's ability to balance high-level deliberative reasoning via the LaST CoT with responsive, high-frequency execution.

1. *Wipe whiteboard.* This task requires the robot to pick up an eraser on the table and clear colored blocks through visual recognition. Success depends on the model's ability to maintain a stable spatial trajectory and ensure the erasing path accurately covers the target blocks.

2. *Press stamp.* The robot is required to establish a stable grasp on a stamp and execute a vertical press onto paper. This task evaluates the model's ability to maintain a consistent execution plan even when the critical contact point is visually occluded during the final press.

3. *Place dish on rack.* This task requires the robot to grasp a plate and perform a large 6-DoF rotation to insert it into a narrow rack. This demands highly accurate spatial perception and the ability to predict complex rotational trajectories for upright placement.

4. *Place egg on bread.* This task requires the robot to pick up the spatula, lift the egg, and place the egg onto the bread. The model must reason about the precise relative positioning

between the spatula tip and the pan to slide under and lift the egg without failure.

5. *Scoop popcorn into bowl.* This collaborative task involves one arm scooping with a bucket while the other arm holds a bowl, then placing the bowl with popcorns on the plate. It validates the model's capacity for precise temporal synchronization and spatial coordination between two independent action streams.

6. *Open pot pick corn.* A long-horizon sequence involving lid removal, object retrieval, and lid replacement. This task evaluates the model's planning depth and collision-avoidance capabilities within a restricted workspace requiring seamless bimanual interaction.